

YAP1 promotes adipogenesis by regulating the negative feedback mechanism of the Hippo signaling pathway via LATS2

Mei Zhou^{1,2}, Yue-Qi Zhao¹, Wei Yan³, Xue-Feng Fu¹, Li-Hui Zhang¹, Hong-Yan Zhang¹, Ge-Gen-Tu-Ya Bao¹, Dong-Jun Liu^{1*}

¹ State Key Laboratory of Reproductive Regulation & Breeding of Grassland Livestock, Inner Mongolia University, Hohhot, Inner Mongolia 010021, China

² College of Coastal Agricultural Sciences, Guangdong Ocean University, Zhanjiang, Guangdong 524088, China

³ Inner Mongolia Key Lab of Molecular Biology, School of Basic Medical Sciences, Inner Mongolia Medical University, Hohhot, Inner Mongolia 010070, China

ABSTRACT

Adipose-derived mesenchymal stem cells (ADSCs) represent a readily accessible and important source of mesenchymal stem cells (MSCs) capable of multilineage differentiation. The Hippo signaling pathway effector YAP has emerged as a pivotal regulator of stem cell fate, yet the specific molecular mechanism by which it modulates lipogenic differentiation of ADSCs has not been clearly defined. In this study, goat ADSCs (gADSCs) isolated from Albas goats in Inner Mongolia were used to investigate the role of YAP1 in adipogenic differentiation. Overexpression of YAP1 significantly promoted the differentiation of ADSCs into adipocytes, an effect accompanied by up-regulation of LATS2 and activation of the negative feedback loop of the Hippo signaling pathway. Elevated LATS2 expression induced YAP phosphorylation, leading to reduced nuclear levels of YAP and TAZ and their subsequent accumulation in the cytoplasm. YAP1 overexpression up-regulated LATS2 expression, which, in turn, enhanced the adipogenic differentiation of ADSCs. This pro-adipogenic effect of YAP1 was dependent on LATS2 kinase activity. These findings indicate that overexpression of YAP1 promotes ADSC adipogenesis by inducing LATS2 expression and activating the Hippo pathway negative feedback loop. Elucidating the molecular role of YAP in ADSC lipogenic differentiation holds great significance for regulating stem cell fate, treating metabolic disorders, and promoting hair follicle growth.

Keywords: ADSCs; YAP1; LATS2; Adipogenesis

This is an open-access article distributed under the terms of the Creative Commons Attribution Non-Commercial License (<http://creativecommons.org/licenses/by-nc/4.0/>), which permits unrestricted non-commercial use, distribution, and reproduction in any medium, provided the original work is properly cited.

Copyright ©2025 Editorial Office of Zoological Research, Kunming Institute of Zoology, Chinese Academy of Sciences

INTRODUCTION

Mesenchymal stem cells (MSCs) are a class of adult stem cells with robust self-renewal capacity and the ability to differentiate into multiple cell lineages (Peister et al., 2004; Pittenger et al., 1999). Among these, adipose-derived mesenchymal stem cells (ADSCs) are particularly valued due to their accessibility, abundance, genetic stability, and multidirectional differentiation potential (Mazini et al., 2019). As a major source of MSCs, ADSCs are widely regarded as ideal candidates for regenerative medicine and stem cell-based therapies (Edgar et al., 2020; Owczarczyk-Saczonek et al., 2017; Puissant et al., 2005; Song et al., 2016). Intradermal white adipose tissue and hair follicles share several overlapping regulatory networks, and signals derived from adipose tissue have been implicated in modulating follicular dynamics. Evidence from knockout mouse models has confirmed the critical role of intradermal white adipose tissue in supporting the hair cycle (Hesslein et al., 2009), underscoring the importance of perifollicular adipose tissue in maintaining follicular microenvironmental homeostasis and cyclical growth. Elucidating the mechanisms governing the adipogenic differentiation of ADSCs is therefore essential for advancing strategies related to stem cell fate control, metabolic disease intervention, and hair follicle regeneration.

Adipocyte differentiation is a complex, tightly regulated process driven by the activation of lipogenic genes under the control of specific lipogenic-related transcription factors. Among the regulators of this process, YAP—a principal downstream effector of the Hippo signaling pathway—has emerged as a critical mediator of cell fate decisions. Ubiquitously expressed across tissues, YAP functions as a transcriptional co-activator of the TEAD family in the nucleus (Oka et al., 2010) and interacts with various proteins that

Received: 11 February 2025; Accepted: 11 March 2025; Online: 12 March 2025

Foundation items: This work was supported by the Joint Fund for Regional Innovation and Development of the National Natural Science Foundation of China (U23A20226) and Science and Technology Planning Project of Inner Mongolia Autonomous Region (2023KYPT0014)

*Corresponding author, E-mail: nmliudongjun@126.com

regulate intracellular signaling pathways (Wu et al., 2025). YAP exists in two metastable shear isoforms, YAP1 and YAP2, as well as an extended variant known as YAP2-L (YAP2-long) (Huang et al., 2005; Komuro et al., 2003; Sudol et al., 1995; Vassilev et al., 2001; Yagi et al., 1999). Due to its lack of a distinct DNA-binding domain, YAP modulates gene expression through interaction with other nuclear transcriptional regulators (Yagi et al., 1999). While YAP has been shown to favor osteogenic over adipogenic differentiation in murine models (Lorthongpanich et al., 2019), its role in regulating adipogenic differentiation in goat-derived ADSCs (gADSCs) remains unclear.

Originally identified through *Drosophila* genetic screens targeting regulators of tissue growth (Udan et al., 2003), the Hippo signaling pathway has since been recognized as a conserved mechanism in both invertebrates and mammals. Various studies have highlighted its critical role in regulating organ size, limiting cell proliferation, and inducing apoptosis (Halder & Johnson, 2011; Pan, 2010; Zhao et al., 2008a; Zheng & Pan, 2019). In mammals, the core components include the serine/threonine kinases MST1/2 and LATS1/2 (Chan et al., 2005). Activation of LATS1/2 leads to phosphorylation of YAP at Ser127, promoting its cytoplasmic retention via binding to 14-3-3 proteins, followed by ubiquitination and proteasomal degradation (Zhao et al., 2010). In contrast, unphosphorylated YAP translocates to the nucleus, where it binds to TEAD family transcription factors, initiating gene expression and stimulating cell activity and proliferation (Zhao et al., 2008b). Despite extensive studies on the mechanisms regulating adipogenesis, the role of Hippo signaling, particularly the function of LATS2, in this context remains underexplored (An et al., 2013; Deng et al., 2019; Gao et al., 2018; Kamura et al., 2018; Li et al., 2018; Zhang et al., 2018). Negative feedback loops are crucial for maintaining signaling equilibrium. Recent studies have identified a feedback mechanism in mammalian cells in which the activation of YAP/TAZ up-regulates LATS1/2 kinases, thereby attenuating YAP/TAZ activity through negative feedback (He et al., 2019; Moroishi et al., 2015; Park et al., 2016; Sun, 2021; Zhang et al., 2022). These observations suggest that the adipogenic effects of YAP1 may depend on the Hippo signaling pathway.

This study investigated the molecular regulatory mechanism by which YAP influences the adipogenic differentiation of ADSCs, with a specific focus on the negative feedback loop between YAP and LATS2. Elucidating this pathway may yield novel insights into stem cell fate determination and hair follicle growth, providing theoretical guidance for MSC differentiation.

MATERIALS AND METHODS

Isolation and culture of ADSCs

ADSCs were isolated from Arbas cashmere goat fetuses at embryonic day 85 (E85). Adipose tissue was collected from the abdominal infra-femoral region, finely minced, and digested with 0.2% collagenase I for 1 h at 37°C. The resulting cell suspension was centrifuged at 1 500 r/min and 25°C for 5 min. The upper adipose layer was discarded, and an equal volume of erythrocyte lysate was added for 25 min, followed by centrifugation at 1 500 r/min and 25°C for 5 min. After discarding the supernatant, ADSCs were cultured in Dulbecco's Modified Eagle Medium (DMEM; Gibco, USA) containing 10% fetal bovine serum (FBS; Biological Industries, USA) and 1% penicillin/streptomycin. The cells were incubated at 37°C

in a humidified incubator with 5% CO₂. Albas goat muscle-derived satellite cells (MDSCs) and hair follicle stem cells (HFSCs) were isolated and characterized using cell culture methods described in previous studies (Li et al., 2022; Yan et al., 2022).

Culture of 293T cells

Human embryonic kidney 293T cells were cultured in high-glucose DMEM (Gibco, USA) containing 10% FBS. Cells were maintained at 37°C in 5% CO₂ and used for viral production.

Induction of adipogenic differentiation in gADSCs

Upon reaching confluence, gADSCs were induced to differentiate into adipocytes. The culture medium was replaced with DMEM containing 3% FBS, 5% rabbit serum (Biological Industries, USA), 33 µmol/L biotin (Sigma, USA), 17 µmol/L pantothenic acid (Sigma, USA), 10 µg/mL insulin (Gibco, USA), 1 µmol/L dexamethasone (Sigma, USA), 5 µmol/L rosiglitazone (Sigma, USA), and 0.5 mmol/L 3-isobutyl-1-methylxanthine (IBMX, Sigma, USA). After 3 days, the induction medium was replaced with maintenance medium lacking IBMX and rosiglitazone, with changes every 3 days.

Lentiviral construction and infection

Lentiviral vectors for YAP overexpression (OE-YAP) and YAP knockdown via short hairpin RNA (shRNA), targeting the sequence 5'-CCGGGCTCAGATCCCTTTCTTAACACTCGAG-TGTTAAGAAAGGGATCTGAGCTTTTTT-3' (sh-YAP), were synthesized by Beijing Tsingke Biotech (China). Lentiviral particles were produced by co-transfecting the Phbv-CMV-Puro vector with packaging plasmids pMD2.G and psPAX2 into 293T cells. After 48 h, the lentivirus-containing culture supernatant was filtered, concentrated, and mixed with 5 mL of lentivirus and 5 mL of complete medium to culture MSCs for 48 h. Puromycin (Sangon Biotech, Shanghai, China) was added at 1 µg/mL for 72 h to select transduced cells, followed by replacement with fresh medium for 24 h. A second round of puromycin selection (1 µg/mL for 72 h) was performed to ensure stable integration.

Oil Red O staining and quantification

Following adipogenic induction, cells were rinsed with phosphate-buffered saline (PBS) and fixed with 4% paraformaldehyde for 15 min. After an additional PBS wash, cells were stained with 3 mg/mL Oil Red O for 1 h at room temperature in the dark. Excess dye was removed by PBS rinsing, and stained lipid droplets were visualized under a light microscope. Subsequently, Oil Red O was discarded, and cells were air-dried. Isopropanol was added to dissolve the lipid droplets, and absorbance was measured at 550 nm to quantify intracellular lipid accumulation.

Immunofluorescence

ADSCs were seeded in 24-well plates at a density of 1 × 10⁴ cells/well and treated with 0.1% gelatin. After incubation for 48 h, cells were fixed in 4% paraformaldehyde at room temperature for 15 min, permeabilized with 0.5% TritonX-100 for 10 min at room temperature, and blocked with 1% bovine serum albumin for 30 min. Primary antibodies were applied and incubated overnight at 4°C, followed by incubation with secondary antibodies conjugated with Alexa Fluor® 488 (Proteintech, China) for 1 h at room temperature. After staining with DAPI (Sigma, USA) for 5 min, the samples were mounted with glycerol and imaged using a confocal laser microscope (Nikon A1 Plus, Japan). Antibodies used are listed in Supplementary Table S1.

Western blot analysis

Total protein was extracted using a mammalian protein extraction kit (CW BIO, China) supplemented with protease inhibitors. Nuclear and cytoplasmic proteins were isolated using a cellular nuclear and cytoplasmic protein extraction kit (CW BIO, China) according to the manufacturer's instructions. Protein concentrations were determined using a BCA protein assay kit (Thermo Fisher Scientific, USA). Proteins (20–30 µg) from cell lysates were separated using sodium dodecyl sulfate-polyacrylamide gel electrophoresis (SDS-PAGE) and transferred to nitrocellulose membranes (Pall, USA). Membranes were blocked with 5% nonfat milk for 1 h at room temperature and incubated overnight at 4°C with primary antibodies. Following three washes, membranes were incubated with horseradish peroxidase (HRP)-conjugated secondary antibodies (Proteintech, China) for 1 h at room temperature. Antigen-antibody complexes were visualized using Pierce ECL western blotting substrate (Thermo Fisher Scientific, USA). Membrane images were captured using a Tanon 5200 imaging system and analyzed with ImageJ software. The primary antibodies used are listed in Supplementary Table S1.

Reverse transcription-quantitative real-time polymerase chain reaction (RT-qPCR)

Total RNA was extracted from ADSCs using RNAiso reagent (Takara, Japan). Complementary DNA (cDNA) synthesis was carried out using the PrimeScript™ RT reagent kit and gDNA Eraser (Perfect Real Time) (Takara, Japan). PCR was performed and detected using the CFX96 Real-Time PCR Detection System. Glyceraldehyde 3-phosphate dehydrogenase (GAPDH) was used as the housekeeping gene, and relative gene expression levels were calculated using the comparative CT method ($\Delta\Delta CT$). Primers used in this study are listed in Supplementary Table S2.

Transcriptomic analysis

ADSCs from OE-YAP and control groups were collected, with three replicates per group. Total RNA was extracted using TRIzol reagent (Invitrogen, USA) according to the manufacturer's protocols. RNA purity and quantification were assessed using a NanoDrop 2000 spectrophotometer (Thermo Fisher Scientific, USA). RNA libraries were constructed using a VAHTS Universal V6 RNA-seq Library Prep Kit and sequenced by OE Biotech (China) on the Illumina NovaSeq 6000 platform (USA) to generate 150 bp paired-end reads. Clean reads were mapped to the reference genome using HISAT2. Gene expression was quantified as fragments per kilobase of exon per million mapped reads (FPKM), and read counts were obtained using HTSeq-count. Principal component analysis (PCA) was performed in R (v.3.2.0) to evaluate replicate consistency. Differential expression analysis was conducted with DESeq2, with significantly differentially expressed genes (DEGs) defined as those with a Q-value <0.05 and a fold change >2 or <0.5. Hierarchical clustering analysis of DEGs was performed using R (v.3.2.0) to visualize gene expression patterns across different groups and samples. Functional enrichment of DEGs was assessed using hypergeometric tests for Gene Ontology (GO), Kyoto Encyclopedia of Genes and Genomes (KEGG), Reactome, and WikiPathways categories in R (v.3.2.0). Column, chord, and bubble plots illustrating significant enrichment terms were generated using R (v.3.2.0).

Statistical analysis

All experimental data were analyzed using SPSS, with

statistical significance set at $P < 0.05$.

RESULTS

Isolation and characterization of ADSCs

To assess the regulatory role of YAP1 in the lipogenic differentiation of adipose MSCs, gADSCs were first isolated and identified according to established protocols (Ren et al., 2012). Lentiviral constructs were used to generate OE-YAP1 and SH-YAP1 cell lines, which were subsequently employed to evaluate the functional impact of YAP1 on gADSC adipogenic differentiation. Transcriptomic profiling of OE-YAP1 and control cells revealed a significant up-regulation of *Lats2*, a core component of the Hippo signaling pathway. YAP activation induced negative feedback within the Hippo pathway, resulting in reduced nuclear localization of YAP and TAZ, restoration of PPAR- γ transcriptional activity, and enhanced lipogenic differentiation. Notably, the pro-adipogenic function of YAP1 was modulated by LATS2 kinase activity, indicating a feedback-dependent mechanism.

Morphological and molecular analyses confirmed the successful isolation of gADSCs. Cells exhibited a long shuttle-shaped or irregular triangular morphology (Figure 1A). Comparative mRNA expression analysis using HFSCs and MDSCs as reference cell types demonstrated significantly higher expression of CD44, CD49d, CD90, and CD105 in gADSCs (Figure 1B). Immunofluorescence staining further confirmed strong expression of CD105, CD49d, CD90, and CD44, and absence of CD34 and CD45 markers, verifying the high purity of gADSCs and excluding endothelial and hematopoietic cell contamination (Figure 1C, D). Oil Red O staining of gADSCs subjected to adipogenic induction for 2, 6, 10, and 14 days showed progressive accumulation of lipid droplets in both size and number over time (Figure 1E). Transcript and protein levels of lipogenic marker genes in ADSCs were examined after 2, 6, 10, and 14 days of induction. Results showed that the expression levels of CEBP- α , PPAR- γ , and FABP4 increased significantly with induction time (Figure 1F, G). These findings confirm the adipogenic capacity of gADSCs and establish a robust model for mechanistic investigation of YAP1-mediated lipogenic differentiation.

YAP1 enhances adipogenic differentiation in gADSCs

gADSCs were cultured in adipogenic induction medium and assessed for YAP1 expression during lipogenesis on days 1, 4, 8, and 12. Both RT-qPCR and western blot analyses demonstrated a time-dependent increase in both YAP1 mRNA and protein levels throughout the induction period (Figure 2A, B), suggesting that YAP1 expression is positively associated with the progression of adipogenesis.

To investigate the functional role of YAP1 in lipogenic differentiation, lentiviral vectors were used to establish gene overexpression and knockdown in gADSCs. Following two rounds of antibiotic selection, stably transfected puromycin-resistant gADSCs were obtained. At 12 days post-induction, OE-YAP1-transduced cells showed significantly higher YAP1 mRNA and protein levels compared to controls (Figure 2C, D), while SH-YAP1 cells displayed significant down-regulation (Figure 2I, J), indicating effective knockdown following transduction. RT-qPCR and western blot assays confirmed stable transduction with the appropriate OE-YAP1 or SH-YAP1 lentiviral vectors.

The impact of YAP1 on adipogenic differentiation was further evaluated by analyzing lipid accumulation. Oil Red O

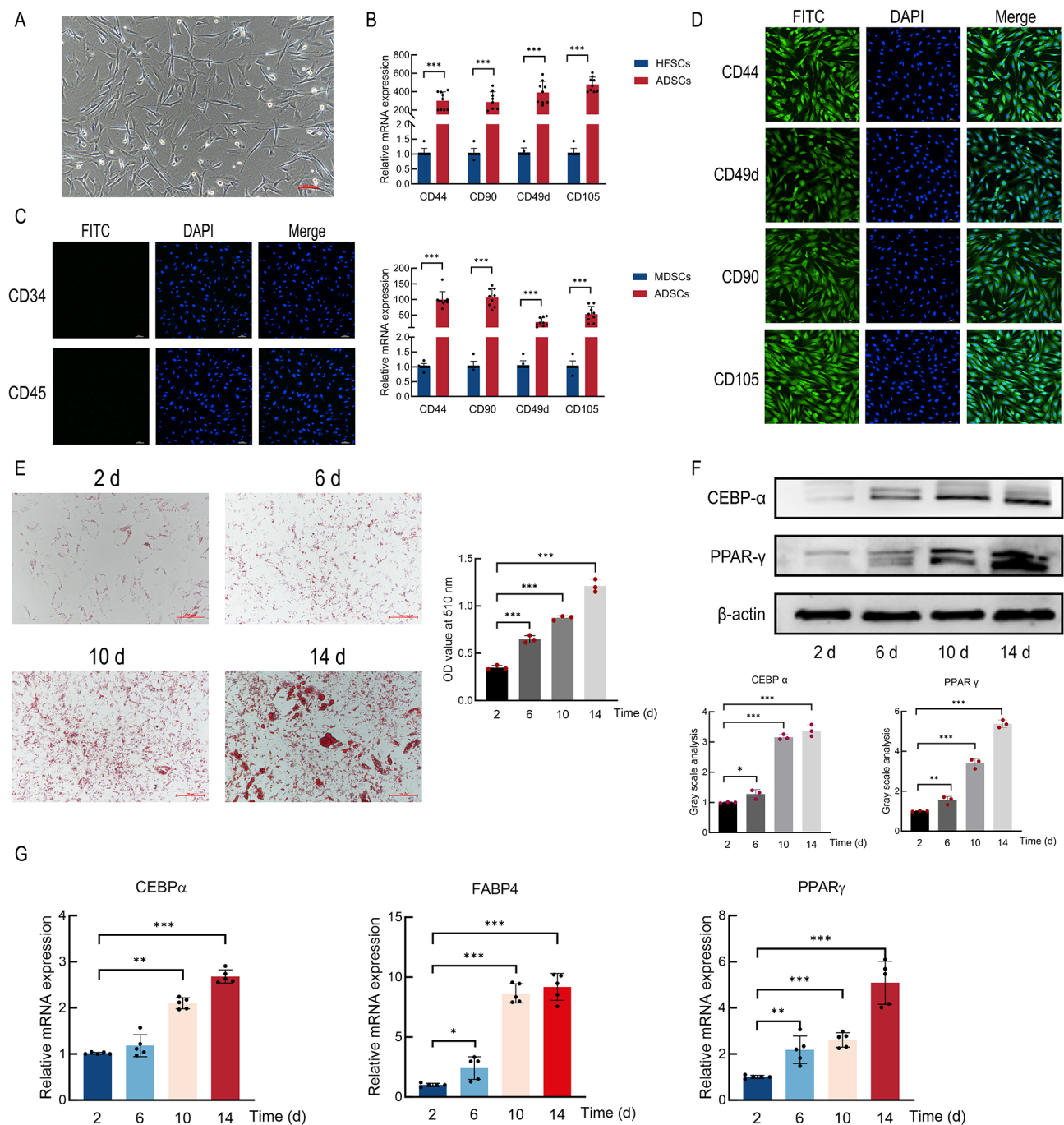


Figure 1 Isolation and characterization of ADSCs

A: Morphology of fourth-generation ADSCs. Scale bar: 100 μ m. B: RT-qPCR analysis of positive markers CD44, CD90, CD49d, and CD105 in ADSCs. C, D: Immunofluorescence staining of cell markers CD44, CD49d, CD90, CD105, CD34, and CD45. Scale bar: 100 μ m. E: Oil Red O staining of ADSCs induced for lipogenesis at 2, 6, 10, and 14 d, with corresponding quantitative analysis. Scale bar: 100 μ m. F: RT-qPCR analysis of PPAR- γ , CEBP- α , and FABP4 expression during lipid induction at 2, 6, 10, and 14 d, normalized to GAPDH. G: Western blot analysis of CEBP- α and PPAR- γ protein expression at 2, 6, 10, and 14 d of lipid induction in ADSCs. All results represent mean \pm standard deviation of three independent experiments ($n=3$). Significant differences compared to the control are indicated. ns: Not significant; *: $P<0.05$; **: $P<0.01$; ***: $P<0.001$.

staining revealed that YAP1 overexpression significantly enhanced lipogenesis on days 8 and 12 of lipogenic differentiation, as indicated by a significant increase in total lipid accumulation (Figure 2F). Quantification was conducted using isopropanol-eluting Oil Red O stain, confirming the enhanced lipid accumulation. To further examine the role of YAP1 in adipogenesis, the expression of adipogenic markers PPAR- γ , CEBP- α , and FABP4 was measured at both the mRNA and protein levels using RT-qPCR and western

blotting. Results showed that OE-YAP1 cells exhibited significantly elevated expression of all three markers (Figure 2E, G, H), supporting a promotive role for YAP1 in adipogenic differentiation of gADSCs. In contrast, YAP1 knockdown resulted in reduced Oil Red O staining on days 8 and 12 (Figure 2L) and decreased PPAR- γ , CEBP- α , and FABP4 expression at both transcript and protein levels (Figure 2K, M, N). Contrary to YAP1 overexpression, YAP1 knockdown inhibited the adipogenic differentiation process.

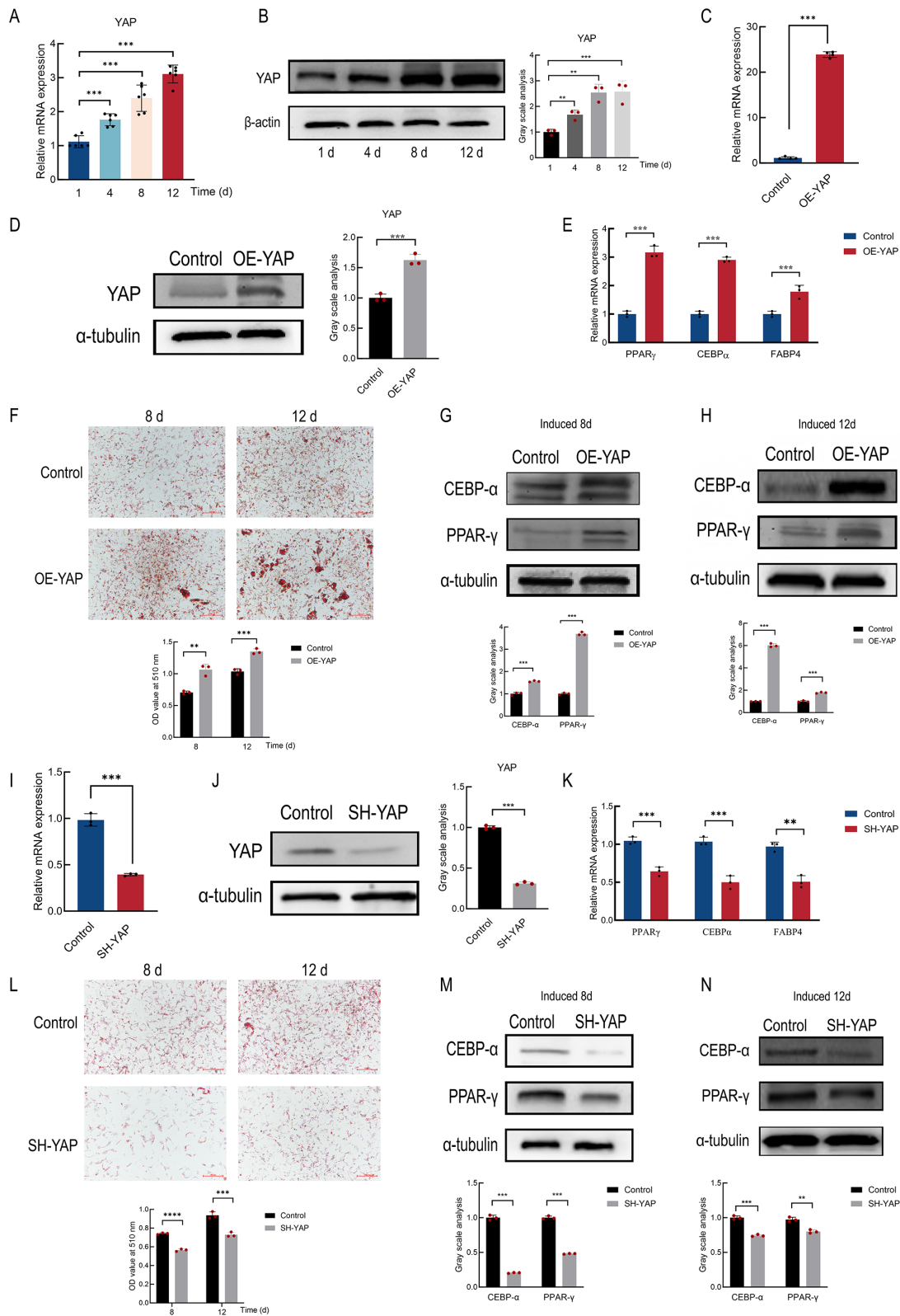


Figure 2 YAP1 promotes adipogenesis in gADSCs

A: RT-qPCR analysis of YAP transcription after 1, 4, 8, and 12 d of lipogenesis induction. B: Western blot analysis of YAP protein expression after 1, 4, 8, and 12 d of adipogenesis induction. C, I: RT-qPCR analysis of YAP1 transcription in gADSCs transfected with OE-YAP1 and SH-YAP1 vectors after 12 d of culture. D, J: Western blot analysis of YAP1 protein expression in gADSCs transfected with OE-YAP1 and SH-YAP1 vectors after 12 d of culture. E, K: RT-qPCR analysis of PPAR-γ, CEBP-α, and FABP4 mRNA levels in OE-YAP1 and SH-YAP1 gADSCs after 12 d of lipid induction. F, L: Oil Red O staining and quantitative analysis of OE-YAP1 and SH-YAP1 gADSCs after 8 and 12 d of lipogenesis induction. Scale bar: 100 μm. G, H, M, N: Western blot analysis of PPAR-γ and CEBP-α protein levels in OE-YAP1 and SH-YAP1 gADSCs after 8 and 12 d of lipid induction. All results represent mean±standard deviation of three independent experiments (n=3). Significant differences compared to the control are indicated. ns: Not significant; *: P<0.05; **: P<0.01; ***: P<0.001.

YAP regulates adipogenic differentiation in gADSCs via the Hippo signaling pathway

Transcriptome sequencing was performed to compare control and OE-YAP1 gADSCs. PCA revealed a clear distinction between OE-YAP1 and control samples (Figure 3A). Differential expression analysis identified a total of 978 DEGs (Figure 3D), including 672 up-regulated and 306 down-regulated genes (Figure 3B, C). To validate the RNA sequencing (RNA-seq) data, 12 DEGs were randomly selected for RT-qPCR analysis. The RT-qPCR results were consistent with RNA-seq-derived FPKM values (Figure 3E), confirming the reliability of the transcriptomic dataset.

GO enrichment analysis of DEGs revealed that most annotations were assigned to biological processes (BP), followed by cellular components (CC) and molecular functions (MF). The DEGs were primarily involved in categories such as cell and cell part (CC), binding and catalytic activity (MF), cellular process, biological regulation and response to stimulus (BP) (Figure 3F). Notably, significant enrichment was observed in fat cell differentiation (GO:0045444), demonstrating an association between YAP1 and lipid differentiation in gADSCs (Figure 3G). KEGG enrichment analysis showed that DEGs were significantly enriched in the Hippo signaling pathway (chx04390). Eight DEGs associated with this pathway were identified, including *WWTR1* (*TAZ*), *Lats1*, *Lats2*, *Mst1*, *TEAD1*, *TEAD2*, *TEAD3*, and *TEAD4*. Expression patterns of these genes are presented in cluster heatmaps (Figure 3J). RT-qPCR analysis confirmed that among these genes, *TAZ* and *LATS2* were significantly up-regulated in OE-YAP cells (Figure 3I), suggesting that YAP1 may promote lipogenic differentiation by modulating *TAZ* and *LATS2* expression through the Hippo signaling pathway. However, further mechanistic studies are required to delineate the precise regulatory cascade.

YAP1 activates negative feedback regulation of the Hippo signaling pathway

YAP1 functions as a transcriptional co-activator recruited by DNA-binding transcription factors to regulate gene expression within the nucleus (Kanai et al., 2000). In MSCs, lineage commitment can be modulated by altering the nuclear localization of YAP1 (Tang et al., 2013). To investigate whether YAP1 localization changes during adipogenic differentiation, its nuclear and cytoplasmic levels were examined on days 1, 4, 8, and 12 of gADSC differentiation. Western blot revealed a gradual decline in nuclear YAP1 levels with increasing differentiation time (Figure 4A), accompanied by a corresponding increase in cytoplasmic YAP1 (Figure 4B), demonstrating that lipogenic differentiation is associated with cytoplasmic redistribution of YAP1.

In OE-YAP1 cells, both YAP and TAZ exhibited reduced nuclear localization and increased accumulation in the cytoplasm, whereas the opposite pattern was observed in SH-YAP1 cells. These results suggest that YAP1 overexpression does not enhance the nuclear translocation of YAP and TAZ but rather decreases their nuclear presence. Consistently, western blot analysis revealed a significant increase in the phosphorylation of YAP (p-YAP) and p-LATS1/2 in OE-YAP1 cells (Figure 4I), while SH-YAP1 cells exhibited reduced phosphorylation (Figure 4J). These findings indicate that YAP1 overexpression activates the Hippo signaling pathway, triggering phosphorylation of LATS1/2. Activated LATS1/2 kinases subsequently phosphorylate YAP, promoting cytoplasmic retention of both YAP and TAZ and reducing their nuclear entry. These observations suggest the presence of an

intrinsic negative feedback mechanism that maintains Hippo pathway homeostasis in gADSCs. Transcriptomic analysis further supported the involvement of the Hippo signaling pathway in YAP1-regulated lipogenic differentiation of gADSCs. Nuclear localization of YAP has been shown to influence adipogenesis (Liu et al., 2020a; Pan et al., 2017; Wang et al., 2020), while TAZ can inhibit this process by binding to and suppressing PPAR- γ activity in the nucleus (Jung et al., 2009). Overall, these findings suggest that YAP1 overexpression promotes adipogenic differentiation by reducing the nuclear presence of YAP and TAZ, thereby relieving their repression of adipogenic transcription factors.

To further investigate the effect of YAP1 on the Hippo signaling pathway, the expression levels of *LATS1* and *LATS2* were examined in OE-YAP1 and SH-YAP1 cells. *LATS1* expression remained unchanged across both cell groups (Figure 4G, I, J), whereas *LATS2* expression was significantly increased in OE-YAP1 cells and significantly down-regulated in SH-YAP1 cells (Figure 4H–J). These results indicate that YAP1 selectively up-regulates *LATS2*, but not *LATS1*, at both the transcript and protein levels, including its phosphorylated form. This suggests that YAP1 activates a *LATS2*-dependent negative feedback loop within the Hippo pathway. Collectively, these findings demonstrate that YAP1 overexpression leads to increased *LATS2* expression and activation, resulting in phosphorylation and cytoplasmic sequestration of YAP and TAZ. This redistribution relieves nuclear repression of adipogenic transcription factors, thereby promoting adipogenic differentiation in gADSCs.

YAP1 promotes adipogenic differentiation of gADSCs via LATS2

Our results suggested that YAP1 enhances adipogenic differentiation by up-regulating *LATS2* expression, thereby activating the negative feedback loop of the Hippo signaling pathway and altering the nuclear abundance of YAP and TAZ. To verify this, a gADSC line stably overexpressing *LATS2* (OE-*LATS2*) was constructed. RT-qPCR and western blot analyses confirmed a significant increase in *LATS2* mRNA and protein levels after 12 d of incubation (Figure 5A, B), indicating successful construction of the OE-*LATS2* line. Following 12 days of adipogenic induction, Oil Red O staining and quantitative analysis demonstrated that OE-*LATS2* promoted lipid droplet accumulation in ADSCs (Figure 5C). Additionally, RT-qPCR and western blot analyses revealed that OE-*LATS2* up-regulated the expression of key adipogenic markers, including *FABP4*, *FASN*, and *ADIPOQ*, at the mRNA level, as well as PPAR- γ and CEBP- α at the mRNA and protein levels (Figure 5D, E). These results indicate that *LATS2* overexpression promotes adipogenic differentiation in ADSCs.

To determine whether *LATS2* promotes lipogenic differentiation through its kinase activity, TRULI (LATS-IN-1), an ATP-competitive inhibitor of *LATS1* and *LATS2* kinases, was added to the gADSC induction solution (Kastan et al., 2022). After 12 days of induction, TRULI treatment significantly reduced lipid droplet accumulation (Figure 5G), suggesting that *LATS2* kinase activity is essential for adipogenesis. A similar reduction in lipid droplet accumulation was observed in OE-YAP1 cells treated with TRULI (Figure 5G). RT-qPCR and western blot analyses further demonstrated that TRULI suppressed the expression of key adipogenic transcription factors, PPAR- γ and CEBP- α , at both mRNA and protein levels. Additionally, TRULI suppressed the increase in PPAR- γ and CEBP- α expression induced by OE-

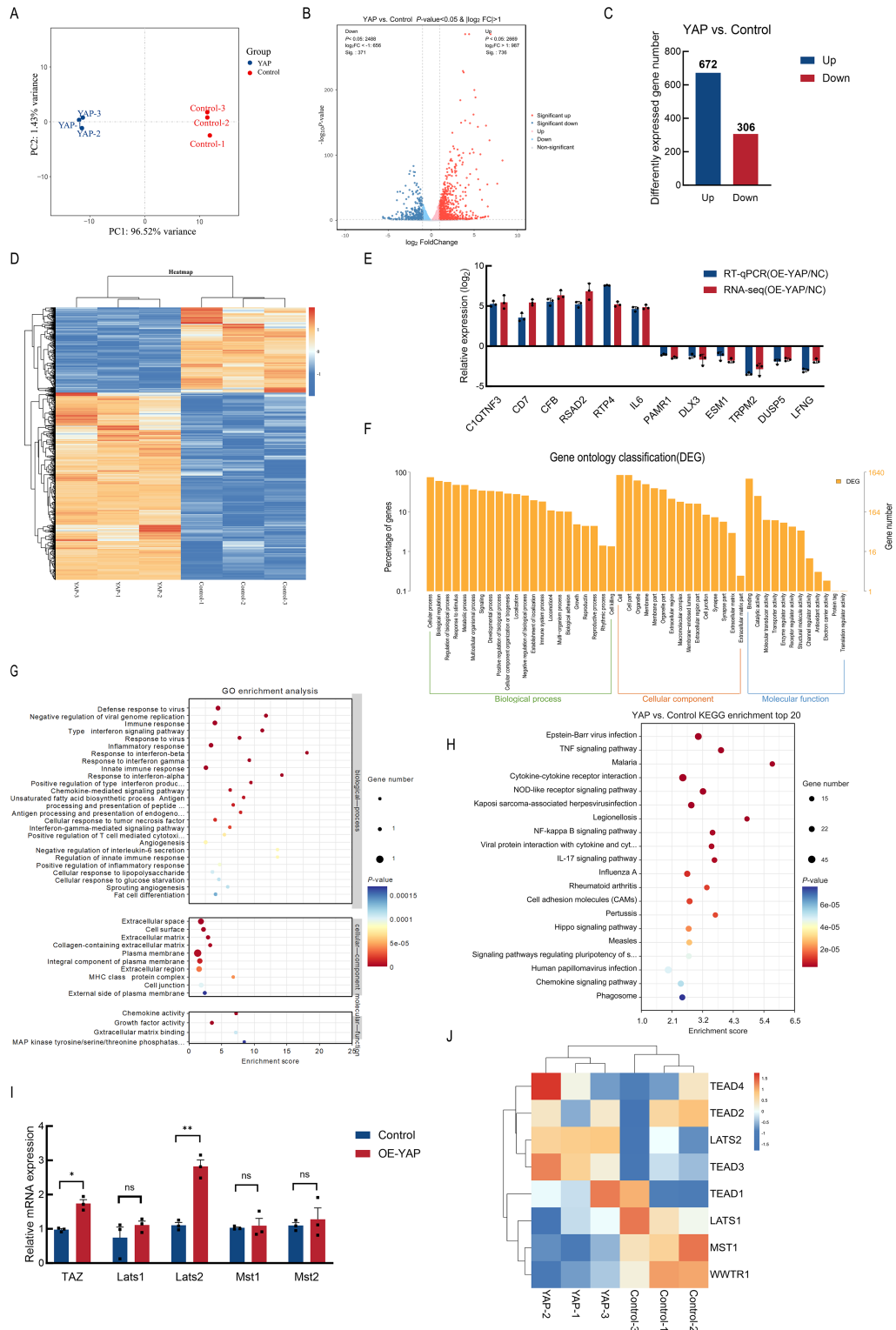


Figure 3 YAP regulates adipogenesis in gADSCs through the Hippo signaling pathway

A: Principal component analysis (PCA) showing separation of gADSCs with OE-YAP1 from untreated gADSCs. Each point represents RNA-seq data for one sample. B: Volcano plot of DEGs in the OE-YAP1 versus control group. X-axis represents Log₂ (fold change); y-axis represents -Log₁₀ (P-value). Red dots indicate up-regulated DEGs; green dots indicate down-regulated DEGs. C: Bar graph showing number of DEGs in the OE-YAP1 versus control group. D: Heatmap of hierarchical clustering showing samples on the horizontal axis and significant DEGs on the vertical axis. E: RT-qPCR validation of DEGs in the OE-YAP1 versus control group. GAPDH was used as an internal control, with each value representing the mean of three independent biological replicates. F: GO functional annotation of DEGs, with term name on the horizontal axis and DEG enrichment on the vertical axis. G: GO enrichment analysis of DEGs. H: KEGG enrichment analysis of DEGs. I: RT-qPCR analysis of transcription of Hippo key genes in OE-YAP cells. J: Heatmap showing clustered expression patterns of key Hippo signaling pathway genes based on transcriptomic data. All results represent mean ± standard deviation of three independent experiments (n=3). Significant differences compared to the control. ns: Not significant; * P<0.05; ** P<0.01; *** P<0.001.

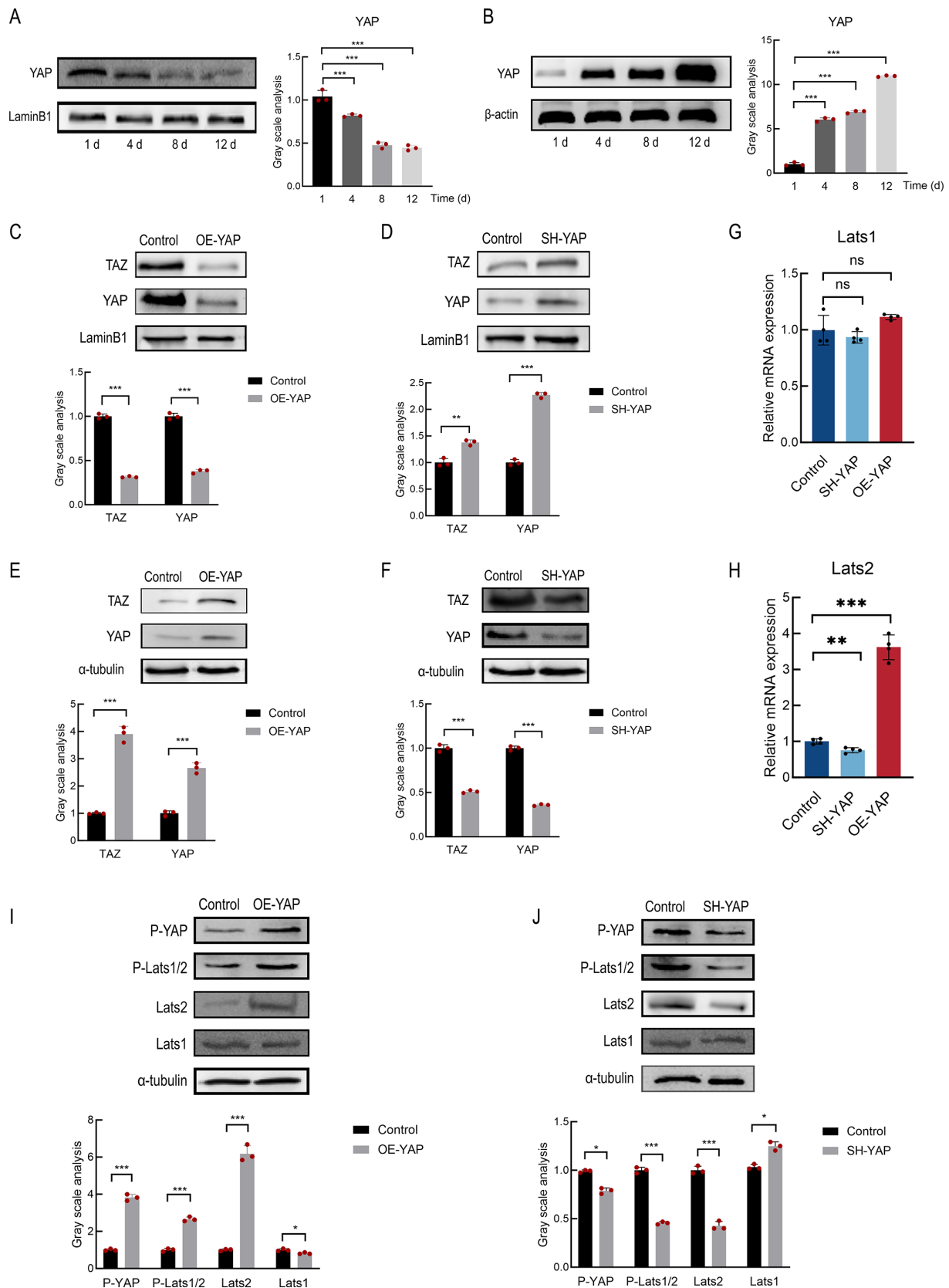


Figure 4 YAP1 activates negative feedback regulation of the Hippo pathway

A: Western blot analysis of YAP1 protein levels in nuclear extracts during lipogenesis at 1, 4, 8, and 12 d of induction. B: Western blot analysis of YAP1 protein levels in cytoplasmic extracts during lipogenesis at 1, 4, 8, and 12 d of induction. C, D: Western blot analysis of YAP and TAZ protein levels in nuclear extracts of OE-YAP1 and SH-YAP1 gADSCs. E, F: Western blot analysis of YAP and TAZ protein levels in cytoplasmic extracts of OE-YAP1 and SH-YAP1 gADSCs. G, H: RT-qPCR analysis of LATS1 and LATS2 transcript levels in OE-YAP1 and SH-YAP1 gADSCs. I, J: Western blot analysis of LATS1, LATS2, phosphorylated YAP, and phosphorylated Lats1/2 protein levels in OE-YAP1 and SH-YAP1 gADSCs. ns: Not significant; * $P < 0.05$; ** $P < 0.01$; *** $P < 0.001$.

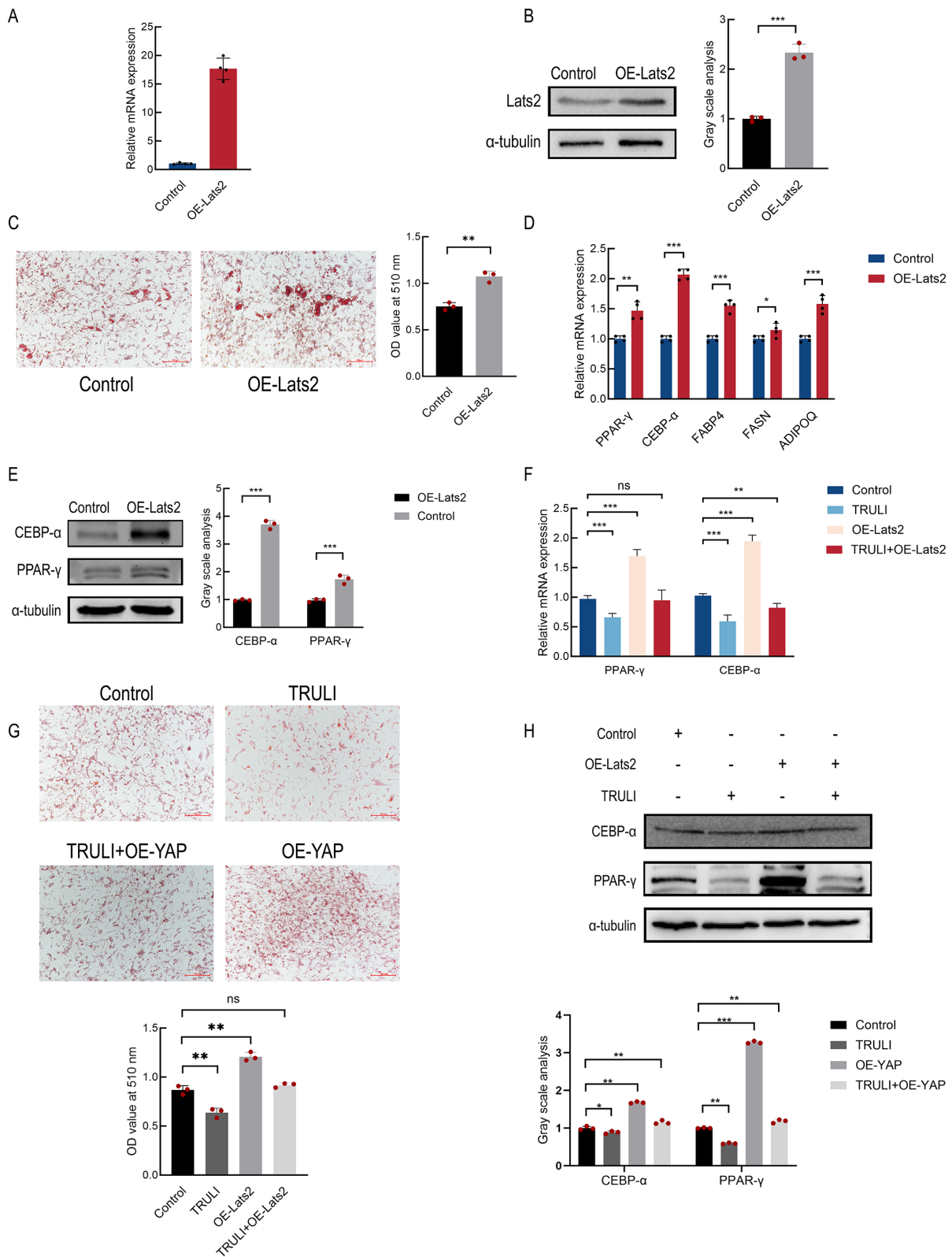


Figure 5 YAP1 promotes adipogenesis of gADSCs via LATS2

A: RT-qPCR analysis of LATS2 transcription in gADSCs stably transfected with OE-LATS2 vector after 12 d of culture. B: Western blot analysis of LATS2 protein levels in gADSCs stably transfected with OE-LATS2 vector after 12 d of culture. C: Oil Red O staining and quantitative analysis of lipid droplet accumulation in OE-LATS2 gADSCs after 12 d of adipogenic induction. Scale bar: 100 μ m. D: RT-qPCR analysis of PPAR- γ , CEBP- α , FABP4, FASN, and ADIPOQ mRNA expression in OE-LATS2 gADSCs after 12 d of lipid induction. E: Western blot analysis of PPAR- γ and CEBP- α protein levels in OE-LATS2 gADSCs after 12 d of lipid induction. F: RT-qPCR analysis of PPAR- γ and CEBP- α expression. G: Oil Red O staining and quantitative analysis of lipid droplet accumulation in control, TRULI, OE-YAP1, and OE-YAP1+TRULI gADSCs after 12 d of lipid induction. Scale bar: 100 μ m. H: Western blot analysis of PPAR- γ and CEBP- α expression. All results represent the mean \pm standard deviation of three independent experiments ($n=3$). Significant difference compared to the control. ns: Not significant; *: $P<0.05$; **: $P<0.01$; ***: $P<0.001$.

YAP1 (Figure 5F, H). These findings suggest that LATS2 promotes adipose differentiation, and that LATS2-kinase inhibitor effectively counteracts the pro-adipogenic effect of OE-YAP1 in ADSCs. YAP1 promotes adipose differentiation in gADSCs by increasing LATS2 expression. This effect is regulated by a negative feedback mechanism in which the Hippo pathway kinase cascade phosphorylates YAP and TAZ, keeping their nuclear concentrations low (He et al., 2019; Moroishi et al., 2015).

DISCUSSION

Stem cell-based therapies have garnered significant attention due to the remarkable self-renewal and multipotent differentiation capacities of MSCs (Kawabori et al., 2020; Li et al., 2020; Liu et al., 2020b). Among them, ADSCs release pro-angiogenic immunomodulatory growth factors and regulatory proteins that support follicular development, wound healing, and related processes through dynamic paracrine signaling (Sumikawa et al., 2014; Won et al., 2012). Efficient induction of adipogenic differentiation is crucial for adipose tissue reconstruction. In particular, dermal white adipose tissue (DWAT), which resides in close proximity to hair follicles and undergoes cyclic remodeling, plays a pivotal role in supporting hair follicle growth and skin regeneration. In addition to regenerative medicine, adipogenesis has important implications for animal production. In livestock, intramuscular and subcutaneous fat content strongly influences meat quality. The Albas cashmere goat, valued for both its high-quality fiber and meat, represents an economically important breed. While studies on human and murine models have explored the role of YAP in ADSC differentiation, research in other species is limited. Therefore, the present study used gADSCs as a model to investigate the molecular mechanisms of adipogenic differentiation in goats. These findings not only expand the species framework for understanding MSC differentiation but also shed light on the molecular regulation of hair follicle development and intramuscular fat deposition in cashmere goats. This study establishes a theoretical foundation for stem cell-based interventions and the advancement of the Albas cashmere and mutton industry.

YAP is widely recognized as a key downstream effector in multiple signaling pathways that govern MSC differentiation (Guo et al., 2018; Tang et al., 2013; Wang et al., 2018). However, few studies have explored the precise mechanism by which YAP regulates ADSC adipogenesis. In this study, stable YAP1 overexpression and knockdown gADSC cell lines were generated using lentiviral transduction to systematically examine the role of YAP1 in lipogenic differentiation. Functional analyses revealed that YAP1 overexpression markedly promoted lipogenesis, while YAP1 silencing attenuated this process. These results are consistent with a positive regulatory role for YAP1 in goat adipogenesis. Interestingly, prior studies in other systems have reported divergent findings. In mouse bone marrow stromal cells, YAP deletion promotes adipogenic differentiation (Pan et al., 2018), while in human periodontal ligament stem cells (hPDLSCs), YAP overexpression reduces adipogenic differentiation (Jia et al., 2019). Such inconsistencies suggest that the function of YAP in adipogenesis may be highly context-dependent, varying across species, cell types, and experimental models. Notably, Qin et al. (2016) reported that both YAP overactivation and suppression impeded adipogenesis in MSCs, and that optimal differentiation required intermediate YAP activity levels. These observations underscore the

complexity of YAP-mediated regulation of adipogenic differentiation, with its role in this process remaining to be fully elucidated.

In 3T3-L1 cells, collagen I activates YAP, increasing its nuclear localization and suppressing lipogenesis (Liu et al., 2020a). Similarly, YAP inactivation promotes osteogenesis and inhibits adipogenesis in rat adipose-derived MSCs, while inhibition of YAP enhances adipogenic differentiation in human MSCs (Jing et al., 2018; Lorthongpanich et al., 2019). These studies suggest that YAP activation impedes adipogenesis. In our study, however, YAP1 interference reduced lipid accumulation, indicating an essential role for YAP1 in promoting adipogenic differentiation in gADSCs. One possible explanation is that YAP1 knockdown triggered compensatory feedback, resulting in nuclear accumulation of YAP1 and inhibition of lipid formation.

Transcriptomic analysis revealed that YAP1 overexpression significantly enriched DEGs within the Hippo signaling pathway and altered the subcellular localization of YAP during lipogenesis. YAP/TAZ activity is tightly regulated through a phosphorylation-dependent inhibitory mechanism. In mammalian systems, a self-regulating negative feedback loop has been identified in which activation of YAP/TAZ up-regulates its own upstream suppressors, LATS1/2 kinases, thereby restricting their nuclear activity and promoting their cytoplasmic sequestration (Hong et al., 2005; Moroishi et al., 2015). This autoregulatory mechanism maintains Hippo pathway equilibrium by limiting excessive YAP signaling. In this study, Hippo pathway activation following YAP1 overexpression resulted in a significant increase in LATS2 expression, along with elevated phosphorylation of both YAP and Lats1/2, in contrast to the effects observed with YAP1 knockdown. Moreover, following YAP1 overexpression, YAP and TAZ progressively accumulated in the cytoplasm while their nuclear levels declined. Conversely, YAP knockdown resulted in increased nuclear localization and reduced cytoplasmic abundance of both proteins. These results indicate that YAP overexpression in gADSCs activates a negative feedback response through the up-regulation of LATS2, which, in turn, phosphorylates YAP, facilitating cytoplasmic retention of both YAP and TAZ and suppressing their nuclear activity.

Within the nucleus, TAZ binds directly to PPAR- γ and suppresses AP2 promoter transcription, while endogenous TAZ-deficiency promotes adipocyte differentiation (Jung et al., 2009; Suh et al., 2012). In mice, YAP has been shown to activate the negative feedback regulation within the Hippo signaling cascade, triggering compensatory suppression of its own activity and that of TAZ, in part through cytoplasmic sequestration. In Yap transgenic mice, down-regulation of TAZ in adipose-derived stem cells activates PPAR- γ , promoting their differentiation into mature adipocytes, thereby increasing adipose tissue (Kamura et al., 2018). In the present study, YAP overexpression activated the Hippo signaling pathway, resulting in the cytoplasmic retention of TAZ and the reactivation of nuclear PPAR- γ , thereby facilitating adipogenic differentiation.

Mechanistically, YAP1 overexpression markedly up-regulated LATS2 expression at both the transcript and protein levels, whereas YAP1 knockdown exhibited the opposite effect. These findings align with previous studies demonstrating that YAP directly induces LATS2 expression as part of a self-limiting feedback loop (Moroishi et al., 2015). To assess the functional relevance of LATS2 in adipogenesis, a gADSC line stably overexpressing LATS2 (OE-LATS2) was

established, which exhibited enhanced adipose differentiation. In contrast, treatment with TRULI, an ATP-competitive inhibitor that selectively targets Lats1 and Lats2 activity and prevents YAP phosphorylation (Kastan et al., 2021), significantly reduced lipid accumulation and inhibited adipose differentiation of gADSCs, diminishing the differentiation-promoting effects of YAP overexpression. YAP1 overexpression in gADSCs increased LATS2 phosphorylation, thereby enhancing YAP phosphorylation and activating the Hippo signaling cascade. To evaluate whether the pro-adipogenic effect of YAP1 overexpression depends on LATS2 kinase activity, LATS2 was inhibited during adipogenic induction. Inhibition of LATS2 suppressed adipocyte differentiation and abolished the adipogenesis-enhancing effect of YAP1 overexpression, indicating that YAP1-driven lipogenic differentiation requires functional LATS2 kinase activity. YAP1 overexpression triggered the Hippo pathway, leading to LATS2 activation and subsequent phosphorylation of YAP1, which promoted cytoplasmic retention of TAZ. This reduction in nuclear TAZ mitigated its repression of PPAR- γ , restoring PPAR- γ transcriptional activity and promoting adipogenic gene expression. When LATS2 activity was inhibited, YAP1 remained unphosphorylated, TAZ accumulated in the nucleus, and PPAR- γ remained repressed, thereby blocking YAP1-induced adipogenic differentiation.

CONCLUSIONS

This study demonstrated that YAP1 overexpression promoted adipogenesis in gADSCs, whereas its suppression yielded the opposite results. YAP1 overexpression enhanced LATS2 expression and activated the Hippo signaling pathway, leading to the phosphorylation of LATS1/2 and YAP. Reduced levels of TAZ in the nucleus restored the activity of the intranuclear transcription factor PPAR- γ and promoted adipogenesis in gADSCs, a process dependent on LATS2 kinase activity. These results provide a deeper understanding of the molecular regulatory mechanisms by which YAP1 influences the adipogenic differentiation of gADSCs. Further studies on the role of ADSCs in maintaining microenvironmental homeostasis of hair follicles and ensuring normal follicular cycling, regulating the balance between adipogenesis and osteogenesis, and advancing applications in regenerative medicine and tissue engineering will provide essential theoretical insights and guide future research directions.

DATA AVAILABILITY

The datasets produced and/or analyzed in the current study are available from the corresponding author upon reasonable request. The raw RNA-seq data analyzed in this study are available from the NCBI database (BioProjectID PRJNA1232596), China National Center for Bioinformatics database of the Genome Sequence Archive (GSA) (CRA023454), and Science Data Bank database (doi: 10.57760/sciencedb.j00139.00179).

SUPPLEMENTARY DATA

Supplementary data to this article can be found online.

COMPETING INTERESTS

The authors declare that they have no competing interests.

AUTHORS' CONTRIBUTIONS

Conceptualization, M.Z.; Methodology, M.Z., G.G.T.Y.B., H.Y.Z., and Y.Q.Z.; validation, M.Z., Y.Q.Z., H.Y.Z., L.H.Z., W.Y., and X.F.F.; Formal analysis, M.Z. and X.F.F.; Writing—original draft preparation, M. Z.; Writing—review and editing, M.Z.; Visualization, M.Z.; Project administration, D.J.L.; Funding acquisition, D.J.L. All authors read and

approved the final version of the manuscript.

ACKNOWLEDGMENTS

We thank members of the Dong-Jun Liu Laboratory for their advice and critical reading of the manuscript. We would like to thank Editage (www.editage.cn) for English language editing.

REFERENCES

- An Y, Kang QQ, Zhao YF, et al. 2013. Lats2 modulates adipocyte proliferation and differentiation via hippo signaling. *PLoS One*, **8**(8): e72042.
- Chan EHY, Nousiainen M, Chalamalasetty RB, et al. 2005. The Ste20-like kinase Mst2 activates the human large tumor suppressor kinase Lats1. *Oncogene*, **24**(12): 2076–2086.
- Deng KP, Ren CF, Fan YX, et al. 2019. YAP1 regulates PPAR γ and RXR α expression to affect the proliferation and differentiation of ovine preadipocyte. *Journal of Cellular Biochemistry*, **120**(12): 19578–19589.
- Edgar L, Pu T, Porter B, et al. 2020. Regenerative medicine, organ bioengineering and transplantation. *British Journal of Surgery*, **107**(7): 793–800.
- Gao SY, Yang DP, Huang W, et al. 2018. miR-135a-5p affects adipogenic differentiation of human adipose-derived mesenchymal stem cells by promoting the Hippo signaling pathway. *International Journal of Clinical and Experimental Pathology*, **11**(3): 1347–1355.
- Guo L, Cai T, Chen K, et al. 2018. Kindlin-2 regulates mesenchymal stem cell differentiation through control of YAP1/TAZ. *Journal of Cell Biology*, **217**(4): 1431–1451.
- Halder G, Johnson RL. 2011. Hippo signaling: growth control and beyond. *Development*, **138**(1): 9–22.
- He CB, Lv XM, Huang C, et al. 2019. YAP1-LATS2 feedback loop dictates senescent or malignant cell fate to maintain tissue homeostasis. *EMBO Reports*, **20**(3): e44948.
- Hesslein DGT, Fretz JA, Xi YG, et al. 2009. *Ebf1*-dependent control of the osteoblast and adipocyte lineages. *Bone*, **44**(4): 537–546.
- Hong JH, Hwang ES, Mcmanus MT, et al. 2005. TAZ, a transcriptional modulator of mesenchymal stem cell differentiation. *Science*, **309**(5737): 1074–1078.
- Huang JB, Wu SA, Barrera J, et al. 2005. The Hippo signaling pathway coordinately regulates cell proliferation and apoptosis by inactivating Yorkie, the *Drosophila* homolog of YAP. *Cell*, **122**(3): 421–434.
- Jia LL, Zhang YP, Ji YW, et al. 2019. YAP balances the osteogenic and adipogenic differentiation of hPDLSCs in vitro partly through the Wnt/ β -catenin signaling pathway. *Biochemical and Biophysical Research Communications*, **518**(1): 154–160.
- Jing XZ, Wang J, Yin WF, et al. 2018. Proliferation and differentiation of rat adipose-derived stem cells are regulated by yes-associated protein. *International Journal of Molecular Medicine*, **42**(3): 1526–1536.
- Jung H, Lee MS, Jang EJ, et al. 2009. Augmentation of PPAR γ -TAZ interaction contributes to the anti-adipogenic activity of KR62980. *Biochemical Pharmacology*, **78**(10): 1323–1329.
- Kamura K, Shin J, Kiyonari H, et al. 2018. Obesity in Yap transgenic mice is associated with TAZ downregulation. *Biochemical and Biophysical Research Communications*, **505**(3): 951–957.
- Kanai F, Marignani PA, Sarbassova D, et al. 2000. TAZ: a novel transcriptional co-activator regulated by interactions with 14-3-3 and PDZ domain proteins. *The EMBO Journal*, **19**(24): 6778–6791.
- Kastan N, Gnedeva K, Alisch T, et al. 2021. Small-molecule inhibition of Lats kinases may promote Yap-dependent proliferation in postmitotic mammalian tissues. *Nature Communications*, **12**(1): 3100.
- Kastan NR, Oak S, Liang R, et al. 2022. Development of an improved inhibitor of Lats kinases to promote regeneration of mammalian organs. *Proceedings of the National Academy of Sciences of the United States of America*, **119**(28): e2206113119.
- Kawabori M, Shichinohe H, Kuroda S, et al. 2020. Clinical trials of stem cell

- therapy for cerebral ischemic stroke. *International Journal of Molecular Sciences*, **21**(19): 7380.
- Komuro A, Nagai M, Navin NE, et al. 2003. WW domain-containing protein YAP associates with ErbB-4 and acts as a co-transcriptional activator for the carboxyl-terminal fragment of ErbB-4 that translocates to the nucleus. *Journal of Biological Chemistry*, **278**(35): 33334–33341.
- Li WN, Yan W, Hao F, et al. 2022. Effects of crotonylation on reprogramming of cashmere goat somatic cells with different differentiation degrees. *Animals*, **12**(20): 2848.
- Li YM, Du JY, Zhu ED, et al. 2018. Liraglutide suppresses proliferation and induces adipogenic differentiation of 3T3-L1 cells via the Hippo-YAP signaling pathway. *Molecular Medicine Reports*, **17**(3): 4499–4507.
- Li ZW, Niu SS, Guo BJ, et al. 2020. Stem cell therapy for COVID-19, ARDS and pulmonary fibrosis. *Cell Proliferation*, **53**(12): e12939.
- Liu XL, Long XY, Gao YF, et al. 2020a. Type I collagen inhibits adipogenic differentiation via YAP activation in vitro. *Journal of Cellular Physiology*, **235**(2): 1821–1837.
- Liu XY, Yang LP, Zhao L. 2020b. Stem cell therapy for Alzheimer's disease. *World Journal of Stem Cells*, **12**(8): 787–802.
- Lorthongpanich C, Thumanu K, Tangkietrakul K, et al. 2019. YAP as a key regulator of adipo-osteogenic differentiation in human MSCs. *Stem Cell Research & Therapy*, **10**(1): 402.
- Mazini L, Rochette L, Amine M, et al. 2019. Regenerative capacity of adipose derived stem cells (ADSCs), comparison with mesenchymal stem cells (MSCs). *International Journal of Molecular Sciences*, **20**(10): 2523.
- Moroishi T, Park HW, Qin BD, et al. 2015. A YAP/TAZ-induced feedback mechanism regulates Hippo pathway homeostasis. *Genes & Development*, **29**(12): 1271–1284.
- Oka T, Remue E, Meerschaert K, et al. 2010. Functional complexes between YAP2 and ZO-2 are PDZ domain-dependent, and regulate YAP2 nuclear localization and signalling. *Biochemical Journal*, **432**(3): 461–472.
- Owczarczyk-Saczonek A, Wocidór A, Placek W, et al. 2017. The use of adipose-derived stem cells in selected skin diseases (vitiligo, alopecia, and nonhealing wounds). *Stem Cells International*, **2017**: 4740709.
- Pan DJ. 2010. The hippo signaling pathway in development and cancer. *Developmental Cell*, **19**(4): 491–505.
- Pan HH, Xie YT, Zhang ZQ, et al. 2017. YAP-mediated mechanotransduction regulates osteogenic and adipogenic differentiation of BMSCs on hierarchical structure. *Colloids and Surfaces B: Biointerfaces*, **152**: 344–353.
- Pan JX, Xiong L, Zhao K, et al. 2018. YAP promotes osteogenesis and suppresses adipogenic differentiation by regulating β -catenin signaling. *Bone Research*, **6**: 18.
- Park GS, Oh H, Kim M, et al. 2016. An evolutionarily conserved negative feedback mechanism in the Hippo pathway reflects functional difference between LATS1 and LATS2. *Oncotarget*, **7**(17): 24063–24075.
- Peister A, Mellad JA, Larson BL, et al. 2004. Adult stem cells from bone marrow (MSCs) isolated from different strains of inbred mice vary in surface epitopes, rates of proliferation, and differentiation potential. *Blood*, **103**(5): 1662–1668.
- Pittenger MF, Mackay AM, Beck SC, et al. 1999. Multilineage potential of adult human mesenchymal stem cells. *Science*, **284**(5411): 143–147.
- Puissant B, Barreau C, Bourin P, et al. 2005. Immunomodulatory effect of human adipose tissue-derived adult stem cells: comparison with bone marrow mesenchymal stem cells. *British Journal of Haematology*, **129**(1): 118–129.
- Qin H, Hejna M, Liu YX, et al. 2016. YAP induces human naive pluripotency. *Cell Reports*, **14**(10): 2301–2312.
- Ren Y, Wu HQ, Zhou XY, et al. 2012. Isolation, expansion, and differentiation of goat adipose-derived stem cells. *Research in Veterinary Science*, **93**(1): 404–411.
- Song Y, Xie XY, Gao Y, et al. 2016. Ultrasound-induced microbubble destruction promotes targeted delivery of adipose-derived stem cells to improve hind-limb ischemia of diabetic mice. *American Journal of Translational Research*, **8**(6): 2585–2596.
- Sudol M, Bork P, Einbond A, et al. 1995. Characterization of the mammalian YAP (Yes-associated protein) gene and its role in defining a novel protein module, the WW domain. *Journal of Biological Chemistry*, **270**(24): 14733–14741.
- Suh JS, Kim KS, Lee JY, et al. 2012. A cell-permeable fusion protein for the mineralization of human dental pulp stem cells. *Journal of Dental Research*, **91**(1): 90–96.
- Sumikawa Y, Inui S, Nakajima T, et al. 2014. Hair cycle control by leptin as a new anagen inducer. *Experimental Dermatology*, **23**(1): 27–32.
- Sun TZ. 2021. Multi-scale modeling of hippo signaling identifies homeostatic control by YAP-LATS negative feedback. *Bio Systems*, **208**: 104475.
- Tang Y, Rowe RG, Botvinick EL, et al. 2013. MT1-MMP-dependent control of skeletal stem cell commitment via a β 1-integrin/YAP/TAZ signaling axis. *Developmental Cell*, **25**(4): 402–416.
- Udan RS, Kango-Singh M, Nolo R, et al. 2003. Hippo promotes proliferation arrest and apoptosis in the Salvador/Warts pathway. *Nature Cell Biology*, **5**(10): 914–920.
- Vassilev A, Kaneko KJ, Shu HJ, et al. 2001. TEAD/TEF transcription factors utilize the activation domain of YAP65, a Src/Yes-associated protein localized in the cytoplasm. *Genes & Development*, **15**(10): 1229–1241.
- Wang L, Wang SP, Shi Y, et al. 2020. YAP and TAZ protect against white adipocyte cell death during obesity. *Nature Communications*, **11**(1): 5455.
- Wang N, Xue P, Li ZY, et al. 2018. IRS-1 increases TAZ expression and promotes osteogenic differentiation in rat bone marrow mesenchymal stem cells. *Biology Open*, **7**(12): bio036194.
- Won CH, Yoo HG, Park KY, et al. 2012. Hair growth-promoting effects of adiponectin in vitro. *Journal of Investigative Dermatology*, **132**(12): 2849–2851.
- Wu SS, Zhao XY, Yang L, et al. 2025. Transcription coactivator YAP1 promotes CCND1/CDK6 expression, stimulating cell proliferation in cloned cattle placentas. *Zoological Research*, **46**(1): 122–138.
- Yagi R, Chen LF, Shigesada K, et al. 1999. A WW domain-containing yes-associated protein (YAP) is a novel transcriptional co-activator. *The EMBO Journal*, **18**(9): 2551–2562.
- Yan W, Hao F, Zhe X, et al. 2022. Neural, adipocyte and hepatic differentiation potential of primary and secondary hair follicle stem cells isolated from Arbas cashmere goats. *BMC Veterinary Research*, **18**(1): 313.
- Zhang C, Li CL, Xu KX, et al. 2022. The Hippo pathway and its correlation with acute kidney injury. *Zoological Research*, **43**(5): 897–910.
- Zhang WX, Xu JJ, Li JH, et al. 2018. The TEA domain family transcription factor TEAD4 represses murine adipogenesis by recruiting the cofactors VGLL4 and CtBP2 into a transcriptional complex. *Journal of Biological Chemistry*, **293**(44): 17119–17134.
- Zhao B, Lei QY, Guan KL. 2008a. The Hippo-YAP pathway: new connections between regulation of organ size and cancer. *Current Opinion in Cell Biology*, **20**(6): 638–646.
- Zhao B, Li L, Tumaneng K, et al. 2010. A coordinated phosphorylation by Lats and CK1 regulates YAP stability through SCF ^{β -TRCP}. *Genes & Development*, **24**(1): 72–85.
- Zhao B, Ye X, Yu JD, et al. 2008b. TEAD mediates YAP-dependent gene induction and growth control. *Genes & Development*, **22**(14): 1962–1971.
- Zheng YG, Pan DJ. 2019. The hippo signaling pathway in development and disease. *Developmental Cell*, **50**(3): 264–282.